
ONLINE SYSTEM FOR ANALYZING CURRENTS IN THE UPPER IONOSPHERE ACCORDING TO SWARM SATELLITE DATA

I.O. Belov 
Geophysical Center RAS,
Moscow, Russia, i.belov@gcras.ru

A.A. Soloviev 
Geophysical Center RAS,
Moscow, Russia, a.soloviev@gcras.ru
Schmidt Institute of Physics of the Earth RAS,
Moscow, Russia

V.A. Pilipenko 
Geophysical Center RAS,
Moscow, Russia, pilipenko_va@mail.ru
Schmidt Institute of Physics of the Earth RAS,
Moscow, Russia

M.N. Dobrovolsky 
Geophysical Center RAS,
Moscow, Russia, m.dobrovolsky@gcras.ru

Sh.R. Bogoutdinov 
Geophysical Center RAS,
Moscow, Russia, shm@gcras.ru
Schmidt Institute of Physics of the Earth RAS,
Moscow, Russia

K.D. Kalinkin
Geophysical Center RAS,
Moscow, Russia, Kirillkalinkin@yandex.ru

Abstract. In this paper, we describe the TeslaSwarm online system [<http://aleph.gcras.ru/teslaswarm>] for visualizing field-aligned currents in the upper ionosphere, using data from Swarm low-orbit satellites. The system provides researchers with a simple and convenient tool for event selection and detailed analysis of currents and electromagnetic fields in the upper ionosphere. The system user can select satellite passages over a given region, visualize the geomagnetic field structure and field-aligned currents, compare the pattern of field-aligned currents with the auroral particle precipitation map, using the OVATION-Prime model, and save the selected parameters in a file in text format. We demon-

strate advantages of the developed system over its foreign analogues. In practice, the collection and pre-processing of raw data for experiments make up about 80 % of all work with data. The proposed online system largely saves the user from the most time-consuming work of choosing the required satellite passage segments and calculating the characteristics of interest from raw measurements.

Keywords: field-aligned electric currents, visualization of field-aligned currents, Swarm satellite data, geomagnetic field structure.

INTRODUCTION

Field-aligned electric currents (FACs) are responsible for the electrodynamic connection between near-Earth space and Earth's ionosphere (Figure 1). This connection plays a key role in developing magnetic storms and substorms, auroras, and other high-latitude phenomena [Wu et al., 2017]. Besides stationary currents of the magnetosphere—ionosphere system, transient FACs can be carried by Alfvén perturbations in near-Earth plasma, which are recorded by ground-based magnetometers as geomagnetic ultralow-frequency (ULF) pulsations [Park et al., 2017]. Geomagnetic disturbances near Earth's surface, generated by rapidly alternating FACs, are responsible for the excitation of geomagnetically induced currents (GICs) in electric power transmission lines (see the review [Pilipenko, 2021]).

An effective method of recording FACs is to measure their magnetic effect with low-orbit satellites [Neubert, Christiansen, 2003; Ritter et al., 2013]. Despite the natural errors in converting the magnitude of magnetic variations into the FAC density, the MAGSAT, Orsted, and CHAMP satellite missions have provided a fairly complete picture of large-scale current systems in the ionosphere [Papitashvili et al., 2002]. Sensitivity of state-of-the-art satellite magnetometers is so high that it

even allows the confident detection of ULF waves with a relative magnitude of magnetic disturbances of the order of several millionths of the external geomagnetic field [Pilipenko, Heilig, 2016].

The Swarm satellite constellation, launched in November 2013, is currently operating in low near-Earth orbit [Friis-Christensen et al., 2006]. A pair of Swarm satellites A and C included in it, spaced by 1.4° in longitude, can combine FACs estimated by different methods [Kervalishvili, Park, 2017]. While the large-scale current structure and its control parameters are quite thoroughly studied, the small-scale current structure and its formation mechanisms remain unclear. Measurements are made by a satellite with a certain frequency (from 1 to 50 Hz in the case of Swarm). Knowing the satellite velocity, we can determine the minimum spatial size of a disturbance whose effect can be recorded in satellite data. In this paper, we analyze 1 Hz data. Since Swarm satellites have the first cosmic velocity (~8 km/s), the minimum spatial scale of the structures under study according to the data from one satellite is larger than 7.5 km, as described in Section 2.5 (FAC analysis). When analyzing data from two neighboring satellites, the spatial scale of the irregularities considered will also be determined by the distance between the satellites (more

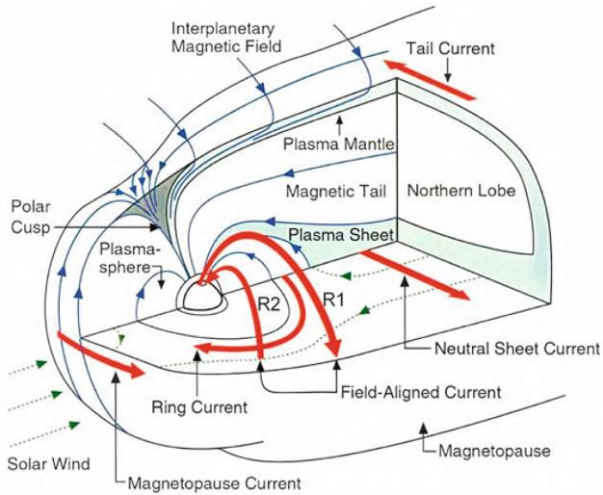


Figure 1. Schematic illustration of Earth's magnetosphere (field-aligned currents are marked with thick red arrows in the center) [Russell et al., 1995]

than 150 km, see Section 2.5, FAC analysis). So, by small-scale we mean structures with a size of the first hundreds of kilometers. Taking into account FACs becomes a necessary element in studying any geomagnetic disturbance or space weather event.

The article describes a new online field-aligned current analysis system TeslaSwarm based on Swarm data — a multifunctional and convenient tool for analyzing currents and electromagnetic fields in the upper ionosphere.

1. GENERAL INFORMATION ON ARCHITECTURE AND SOFTWARE-BASED VISUALIZATION METHODS

The TeslaSwarm online system is freely available [http://aleph.gcras.ru/teslaswarm]. It is a multifunctional service for simultaneous analysis of ground-based

geomagnetic data and data from Swarm satellites. The system makes it possible for any given time interval to visualize a geomagnetic disturbance, FAC magnitude for a selected satellite, and their related ground response, as well as to create on demand text files with selected data for further work outside the system. The general architecture of the system is shown schematically in Figure 2.

Web part is based on the Django web framework and the Apache web server. The rest of the back-end code is written in Python-3.7. The client—server interaction is as follows. A client on the web page [http://aleph.gcras.ru/teslaswarm] enters the parameters of interest and sends a request for data as an image or a text (Figure 3). The front-end, written in JavaScript, generates a query string with parameters specified on the page and sends it to the server, which, in turn, forwards it to Django's HttpRequest. Control logic in views.ru processes the request and from the parameters specified by the client runs internal scripts in the back-end. Django interacts with the Apache web server via UWSGI, which is a binary implementation of WSGI (Web Server Gateway Interface). It is optimized to speed up the server-application interface. After implementing the scripts on the back-end side of the server and converting the required data into text or jpeg image, the Django framework returns the result back to the client in the browser window via HttpResponse. On the back-end side, the Python programming language is generally used.

The Swarm satellite constellation data the online system employs is downloaded from the hardware and software complex (HSC) MAGNUS (Monitoring and Analysis of Geomagnetic aNomalies in Unified System) [Gvishiani et al., 2016], which is the intellectual heart of the Shared Research Facility “Analytical Geomagnetic

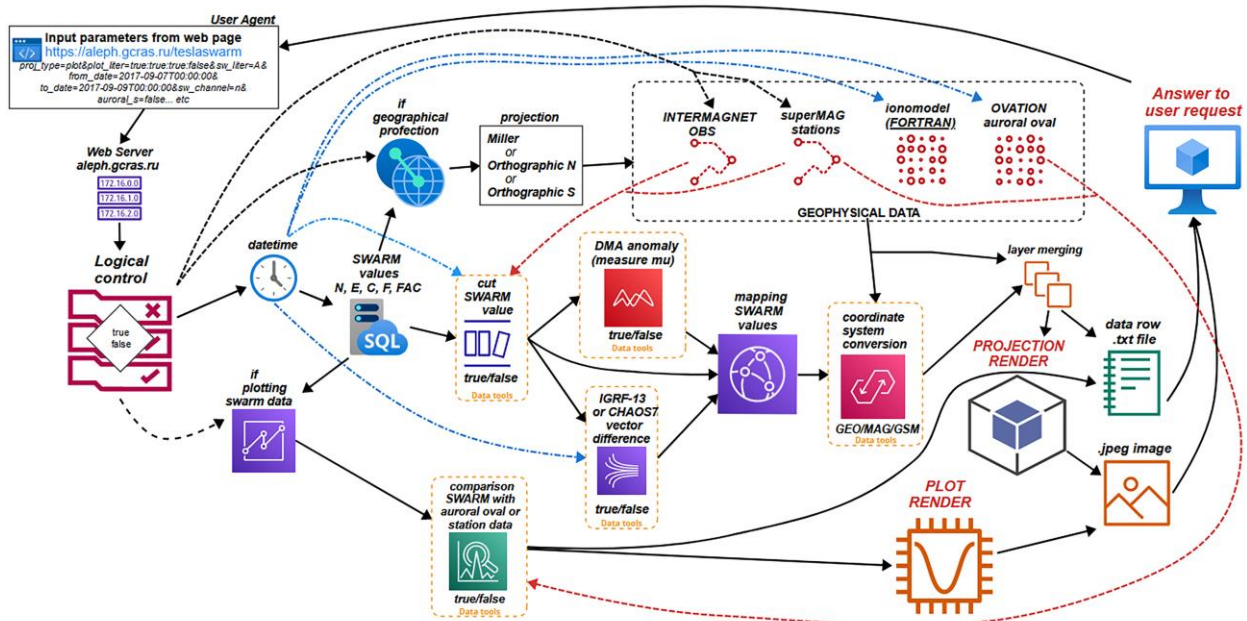


Figure 2. Architecture of the TeslaSwarm online system. Flowchart

Онлайн система для визуализации и анализа данных измерений продольных токов на спутниках SWARM

Выберите тип проекции (Miller, Orthographic north, Orthographic south) или отображение графика (plot)

Выберите литер интересующего спутника SWARM, значения по ротору В J2 на двух близких спутниках А и С (FAC only), или же величину вектора разности SWARM-A и SWARM-C (A-C)

с даты UTC

по дату UTC

Трёхкомпонентные значения магнитного поля (N, E, C), полный вектор магнитного поля (F), плотность продольного тока (FAC)

средний интервал, в секундах

Отображать минутные временные отметки пролета спутника SWARM

Если требуется отображение пролета спутника рядом с обсерваторией INTERMAGNET, выберите ее код и введите радиус в градусах, в пределах которого требуются значения пролета спутников SWARM

obs_code

Отображение значений станций superMAG

superMAG

Если требуется отображение модели Ovation Prime (<https://doi.org/10.1029/2009JA014326>), введите дату и выберите полусферу (north и/или south)

auroral_n

auroral_s

Если требуется увеличение проекции до определенного прямоугольника, введите широту (lat) и долготу (lon)

min_lon max_lon min_lat max_lat

Отображение разности векторов продольных токов между реальными данными, полученные со спутника SWARM и модели CHAOS-7

Отображение разности векторов продольных токов между реальными данными, полученные со спутника SWARM и модели IGRF-13

Поворот вектора магнитного поля в систему вдоль B0

ДМА мера аномальности значений пролета спутника SWARM

Отображение геомагнитной сетки координат

Перевод в геомагнитную сетку

Geophysical Center of Russian Academy of Sciences (GC RAS) © 2022
contact: i.belov@gcras.ru

Figure 3. Client interface for entering parameters and making a request to the online system TeslaSwarm

Data Center” of the Geophysical Center of RAS [<http://ckp.gcras.ru>]. The Python pymysql library [<https://pypi.org/project/PyMySQL/>] is responsible for the connection and import from SQL (Structured Query Language) tables of MAGNUS. MAGNUS receives data from the ftp server of the European Space Agency (ESA) of the Swarm mission [<ftp://swarm-diss.eo.esa.int>]. Below are the parameters of the Swarm satellite constellation orbits:

- Swarm A: orbit perigee is ≤ 460 km, orbit apogee is ≤ 460 km, orbit inclination is 87.4° ;
- Swarm B: orbit perigee is ≤ 530 km, orbit apogee is ≤ 530 km, orbit inclination is 88.0° ;
- Swarm C: orbit perigee is ≤ 460 km, orbit apogee is ≤ 460 km, orbit inclination is 87.4° .

The MAGNUS database stores satellite data with a time resolution of 1 Hz. Resolution of satellite magnetometers in the range from a constant field to 100 Hz is $1 \text{ pT}/\sqrt{\text{Hz}}$. The data format is

- time, UTC;
- Position of the vector magnetometer VFM in spherical geocentric coordinates: geographic latitude, longitude, distance to the geocenter (m);
- three components of the magnetic induction vector B_{NEC} (nT) in the local coordinate system depending on satellite position: N — the northern component, E — the eastern component, C — the vertical component;
- modulus of the magnetic induction vector F (nT)

measured by a scalar magnetometer;

- density of field-aligned currents as measured by individual satellites;
- density of field-aligned currents as measured by Swarm A and C.

2. THE MOST IMPORTANT FUNCTIONALITY OF THE SYSTEM

2.1. Data query and visualization

TeslaSwarm provides a wide range of tools for visualizing and analyzing raw geomagnetic measurements, data derived from them, and auxiliary electromagnetic parameters of near-Earth space. For any user-defined moment/time interval, the following is provided:

- visualization of geomagnetic field measurement data with Swarm A, B, C;
- visualization of the position and parameters of the auroral oval according to the OVATION-Prime model [<https://ccmc.gsfc.nasa.gov/models/Ovation-Prime> ~2.3; Vorobeв et al., 2022];
- comparison with the data from ground-based magnetic stations loaded from the SuperMag portal [<https://supermag.jhuapl.edu>], using the SuperMag Web Service API Python library [Gjerloev, 2012];
- comparison of satellite observations with the geomagnetic field models IGRF-13 [Alken et al., 2021],

using the Python library [https://pypi.org/project/igrf], or CHAOS-7 [Finlay et al., 2020], using the Python library [https://pypi.org/project/chaosmagpy].

The system provides visualization of the parameters of interest in the form of time and coordinates, as well as in the form of a graph along the satellite path projected onto Earth's surface. For the latter case, two projections are available to the user: Miller (for middle and low latitudes) and orthographic (for circumpolar latitudes). Here, the spatial reference of the measurements can be represented both in the projection of the satellite position onto Earth's surface and in the projection of the point of intersection between the field line, related to the satellite position, and the lower edge of the ionosphere (100 km above Earth's surface). The latter option is used when the user needs to know where the disturbance, carried by field aligned currents along the field line and recorded by the satellite, occurs on Earth (for example, to correctly compare with ground magnetometer data). To obtain information about the field line position, the T89 model is used [Tsyganenko, 1989]. When visualizing data in map projections, the solar terminator is drawn, which provides the user with important information about the current position of Earth relative to the Sun, the location of local time zones, and the illumination of the ionosphere.

When the user specifies the ground station of interest, the system can search for all available satellite passages within a given distance and calculate the required parameters along them. This function is useful when it is necessary to compare ground and satellite observations of the magnetic field for a selected period of time (Figure 4, *a*). In panel *b*, a red asterisk marks the position of the magnetic station T47 (SALU) according to the SuperMag database. Direction of satellite motion along its ground path is shown by arrows with time marks (in UT) in increments of 1 min for a given time interval of less than 30 min. It can be cropped to explicit coordinates.

Different problems require the capability of converting satellite vector data from one local coordinate system to another. The most popular systems include geographic (GEO), geomagnetic (MAG), geocentric solar magnetospheric (GSM), and the mean-field aligned (MFA). The last one at each given point is oriented along the large-scale magnetic field vector $\mathbf{B}(t)$. It is in this system that FACs are correctly identified. Depending on the user's interest in the time scale of the disturbance considered, the necessary parameters of the space-time averaging of satellite measurements of $\mathbf{B}(t)$ are set. As a result, the system recalculates to a coordinate system oriented relative to the averaged field. For example, averaging the field in a 100 s running time window corresponding to ~ 800 km of passage allows us to record fluctuations with periods of the order of several tens of seconds against its background. Thus, the user can also assess the contribution of the magnetosonic mode, associated with the magnetic field compression, to perturbation of the Alfvén mode carrying the field-aligned current.

2.2. Analysis of field-aligned currents

The FAC density calculation, provided by the European Space Agency among L2 products of the Swarm

mission, is performed in two ways. Hereinafter, by J_1 and J_2 we mean the field-aligned currents calculated by different algorithms.

The first method involves calculating J_1 from $\text{grad}\mathbf{B}$, measured by an individual satellite with 1 s sampling [Forsyth et al., 2017]. At r , the unit vectors of measuring the magnetic field NEC are equal to [Tøffner-Clausen, 2021]

$$\mathbf{e}_C = \frac{-r}{|r|},$$

$$\mathbf{e}_E = \begin{cases} \frac{a}{|a|}, a = \mathbf{e}_C \times (0\ 0\ 1)^T \\ (0\ 1\ 0)^T, \text{ if } |a| = 0 \end{cases}, \quad (1)$$

$$\mathbf{e}_N = \mathbf{e}_E \times \mathbf{e}_C.$$

Time series of the FAC density are determined by multiplying the radial current density by the angle of geomagnetic field inclination [Kervalishvili, Park, 2017]. In general, the vertical current density formula has the form

$$j_z = \frac{1}{\mu_0} \left[\frac{\partial B_y}{\partial x} - \frac{\partial B_x}{\partial y} \right], \quad (2)$$

where j is the current density; μ_0 is the magnetic permeability; B_x , B_y are transverse magnetic field components (the X-axis is northward; the Y-axis, eastward; and the Z-axis, vertically downward). Assuming that the current sheets are infinitely elongated in the zonal direction, the second term of the right side of the equation can be neglected. Then for the field-aligned current density, (2) takes the form

$$j_{\text{FAC}} = -\frac{j_{\text{IRC}}}{\sin I}, \quad (3)$$

where j_{IRC} is the radial current component according to data from one satellite in view of the above assumptions; I is the magnetic inclination. Near the magnetic equator and at latitudes above 86° , FAC is not estimated. The radial current density is determined along the entire orbit, the spatial scale is larger than 7.5 km, the measurement accuracy is $10^{-6} \mu\text{A}/\text{m}^2$ [Swarm Level-2 Processing System Consortium, 2019].

The second method is to calculate J_2 from $\text{rot}\mathbf{B}$, measured by two neighboring satellites, Swarm A and C, from 1 s data [Dunlop et al., 2015; Lühr et al., 2015]. The FAC density can be calculated only at high latitudes, where the magnetic field is more vertical, i.e. $I > 30^\circ$. At lower geomagnetic latitudes, the time series is not defined. The radial current density can be calculated throughout the orbit, except for $\theta > 86^\circ$ [Lühr et al., 2020]. Its spatial scale is larger than 150 km; the measurement accuracy is $10^{-6} \mu\text{A}/\text{m}^2$. This accuracy satisfies the characteristics of onboard magnetometers, which, in turn, are given in the specification of L2 products [Swarm Level-2 Processing System Consortium, 2019, page 97]. The geographical reference of the values corresponds to the

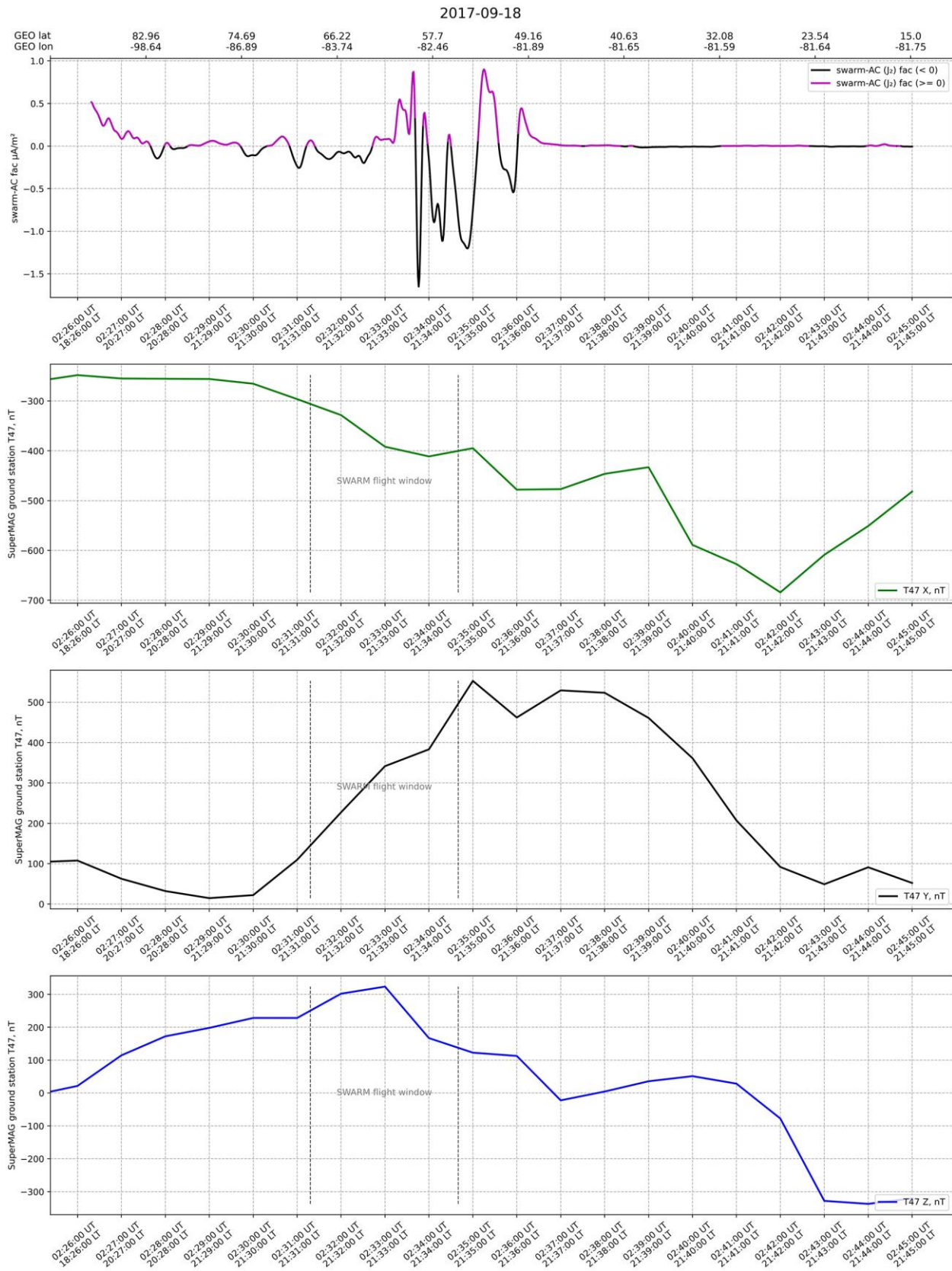


Figure 4. a. FAC density as measured by Swarm A, C on September 18, 2017, from 02:26:00 to 02:45:00 UT. At the top are positive and negative values (pink and black segments of the curve); three magnetic field components (x, y, z) from the T47 station (SALU) for the same time interval (three bottom panels). Vertical dashed lines are the boundaries of the intersection of a region 10° in radius from the station. Hereinafter, examples are generated by the TeslaSwarm online system

J₂, 2017-09-18 02:25:00 -- 2017-09-18 02:45:00

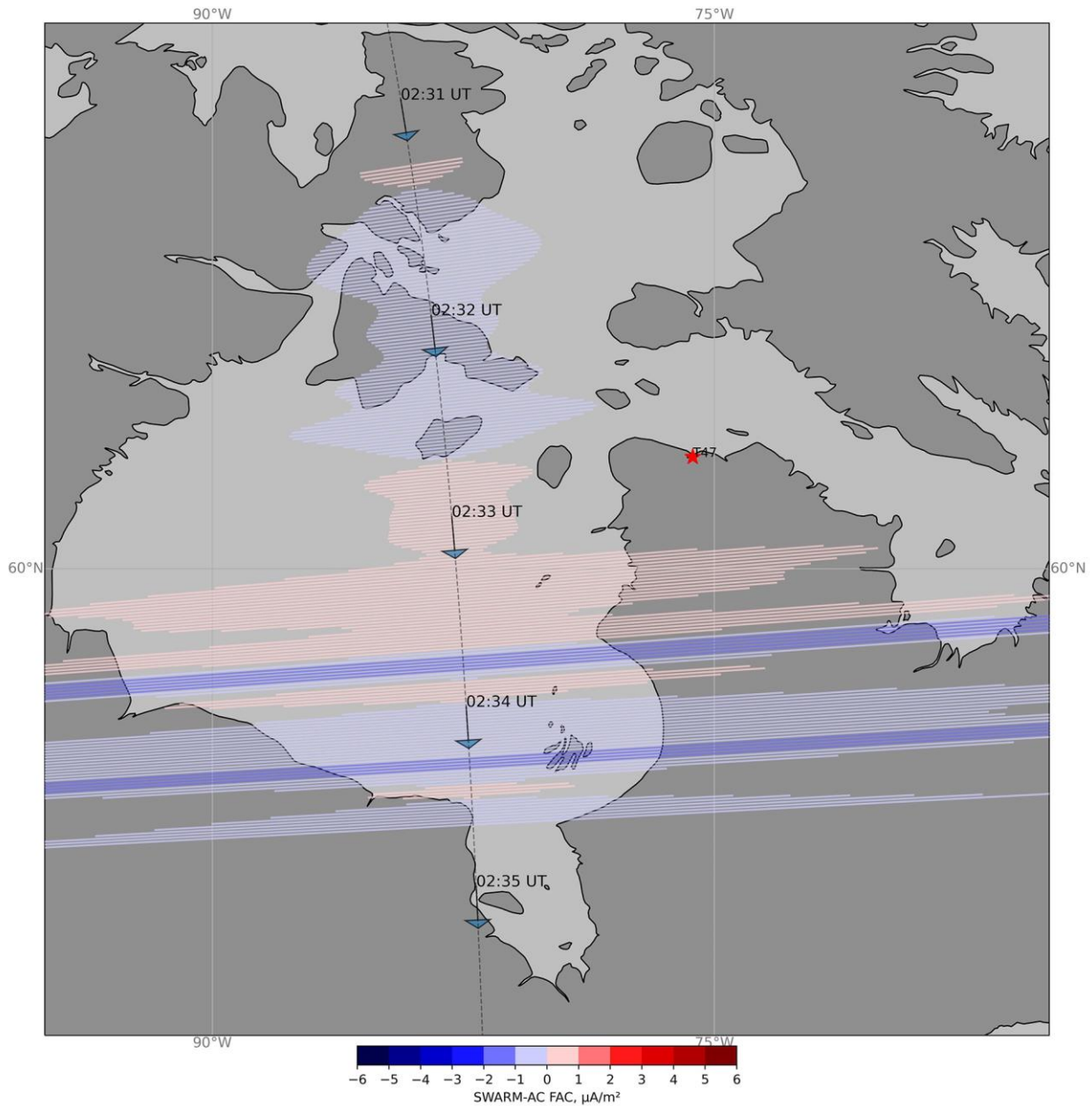


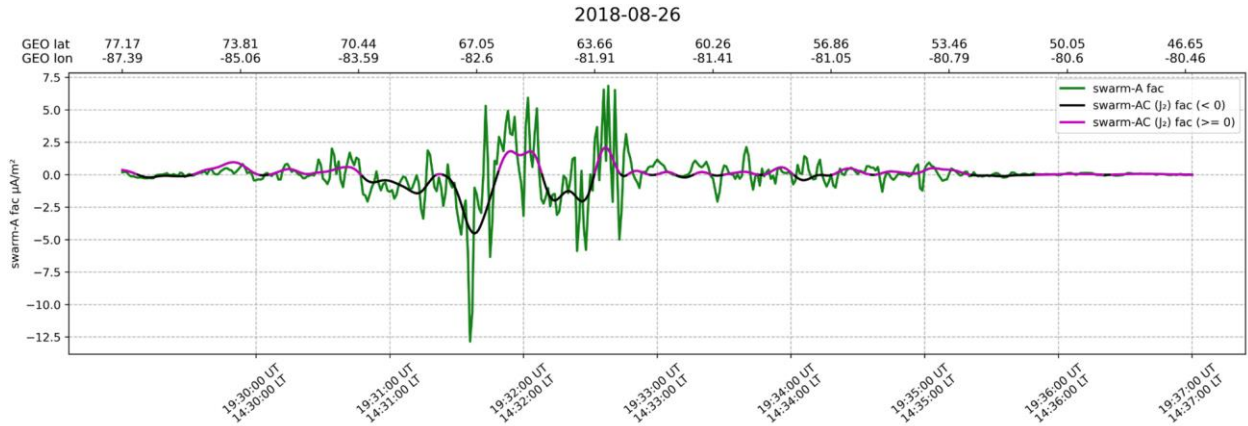
Figure 4, b. Averaged flight path of Swarm A and C (dashed line) with arrows indicating direction of their motion; FAC density along their flight paths, plotted symmetrically to the motion path (color indicates the sign; the length of perpendicular lines, the amplitude). The red asterisk is the position of the T47 station (SALU). Boundaries of the region displayed on the map are set by the user.

averaged orbit of Swarm A, C. Figure 5 exemplifies the visualization of the FAC density, calculated in two ways, as a function of time and coordinates (top) and as a projection on Earth's surface (bottom). The values of currents and fields for the selected time interval can be written to the output text file in tabular form: columns are separated by a space; the first two rows contain a description of the data.

2.3. Comparison between FAC and auroral oval

The OVATION-Prime (OP) model yields a plane-

tary distribution of the intensity of precipitating auroral particle fluxes in geographic coordinates [Newell et al., 2014]. Increased values of these fluxes indicate the auroral oval position. The model is parameterized by interplanetary magnetic field and solar wind characteristics. The corresponding values for the time moment considered are automatically loaded from the OMNIweb database [<https://omniweb.gsfc.nasa.gov/>]. It is assumed that in the time period during which the satellite crosses the auroral oval (~5 min) its configuration does not change. In the current version of the model, particle fluxes to the Northern and Southern hemispheres are averaged,



J_2 , 2021-04-17 09:06:00 -- 2021-04-17 09:26:00

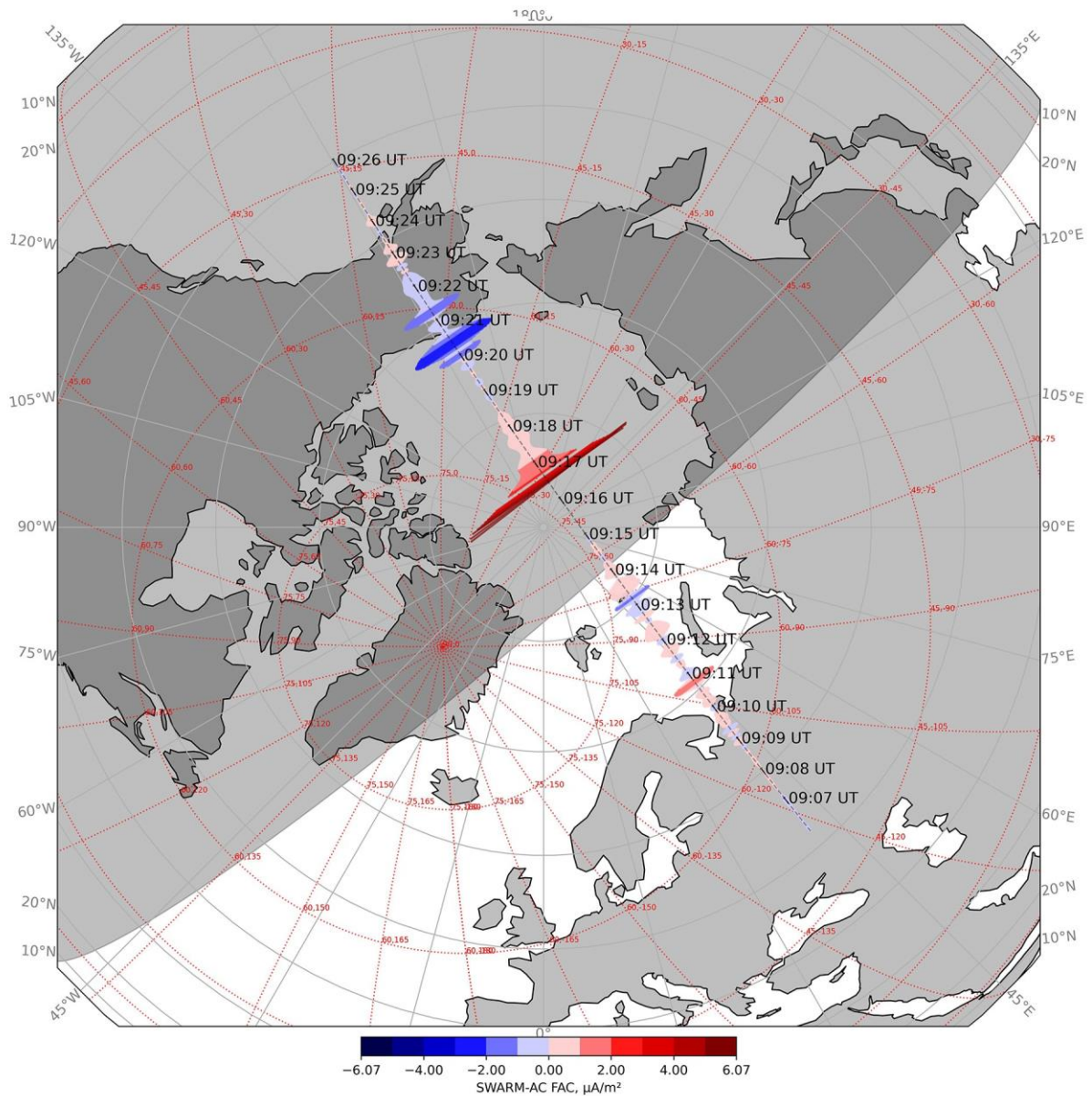


Figure 5. Comparison of J_1 as measured by Swarm A (green line) with J_2 as measured by two neighboring satellites, Swarm A and C, on August 26, 2018, at 19:29–19:37 UT (top); J_2 along the averaged flight of Swarm A and C on April 17, 2021 at 09:06:00–09:26:00 UT in the northern orthographic projection (bottom). Red dotted lines denote parallels and meridians in the geomagnetic dipole coordinate system

J₁, 2021-04-17 09:06:00 -- 2021-04-17 09:26:00

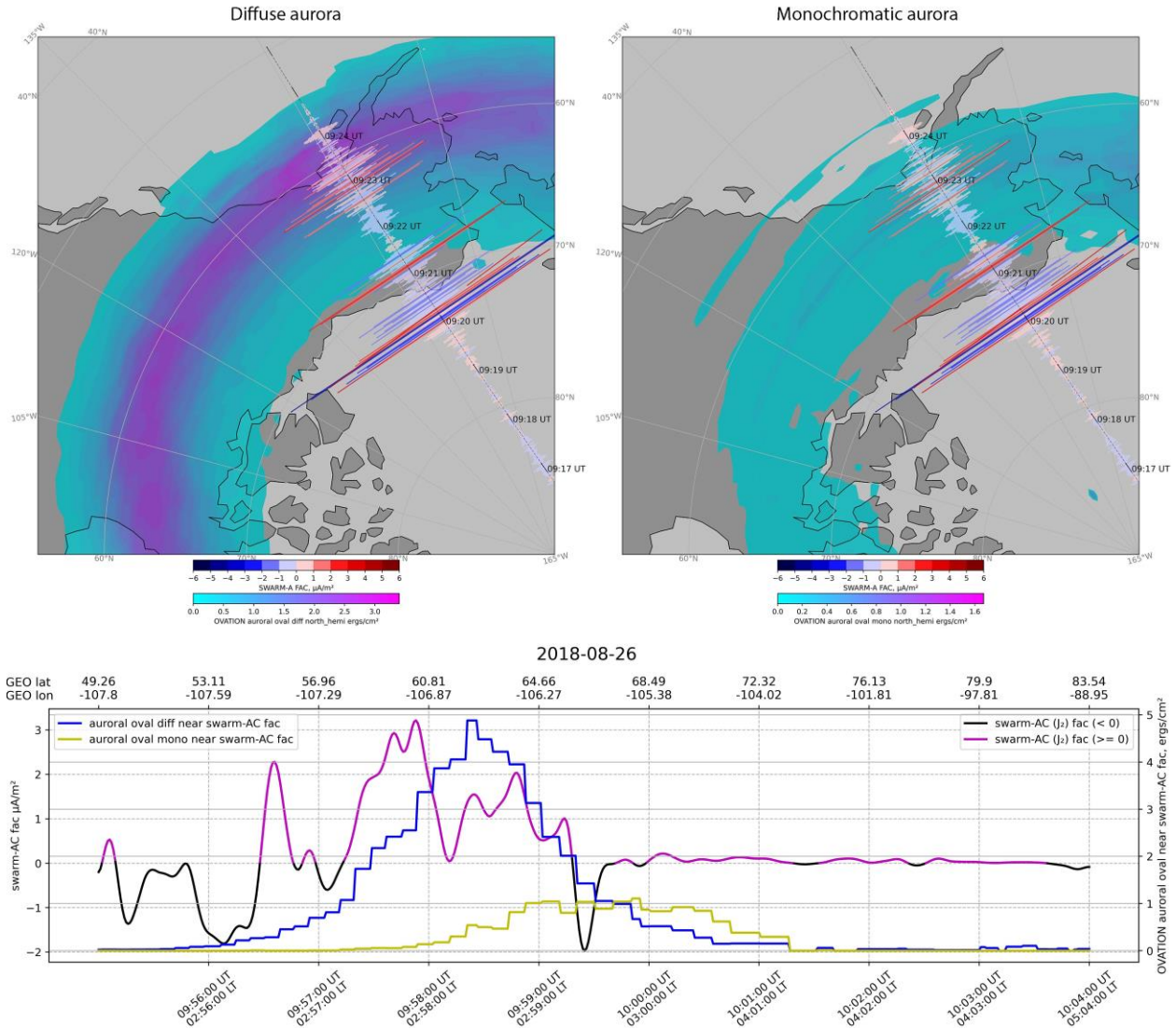


Figure 6. Values of J_1 as measured by Swarm A along its path on April 17, 2021 at 09:06–09:26 UT (blue-red color) in the user-selected region in the northern orthographic projection; auroral particle precipitation intensity for 09:16 UT on April 17, 2021 (turquoise-violet field): diffuse aurora (left), monoenergetic aurora (right) (top); comparison of J_2 (violet-black color) according to Swarm-A data on August 26, 2018 at 09:55:00–10:04:00 UT with the auroral particle precipitation intensity along the satellites' flight paths (bottom). The blue curve is the intensity of auroral particle fluxes along the satellites' flight paths (bottom) for diffuse aurora; the yellow one, for monoenergetic aurora

which allows us to avoid data gaps and smooth possible effects of asymmetry between the hemispheres. The auroral oval model provides spatial distribution of energy fluxes and electron fluxes of different energies responsible for auroras of all possible types [Machol et al., 2012], but the developed web system uses only precipitation of the main types peculiar to discrete and diffuse auroras. FACs measured together with the auroral oval position for the corresponding time interval are exemplified in Figure 6 (top panels). As expected, the auroral oval boundaries coincide with FAC bursts [Zanetti et al., 1998].

2.4. Analysis of perturbed vector field

To identify localized spatio-temporal variations from external sources from satellite measurements and analysis, it is necessary to take into account the contribution of the main geomagnetic field. The system implements

the calculation of parameters of the main field in accordance with the models IGRF [Alken et al., 2021] and CHAOS-7 [Finlay et al., 2020] for each point of passage for the epoch considered. As a result of subtracting the main field from satellite observations, the user can work with the perturbed component of the observed field in the horizontal projection $\Delta\mathbf{B}=\{\Delta N, \Delta E\}$. Figure 7 displays a perturbed vector field along the satellite's ground projection (top panel) and a perturbed vector field in the MFA coordinate system (bottom panel).

2.5. Identification and classification of anomalies in time series

To identify perturbations calculated along the satellite orbit in time series and classify them according to the degree of anomaly, we can use discrete mathematical

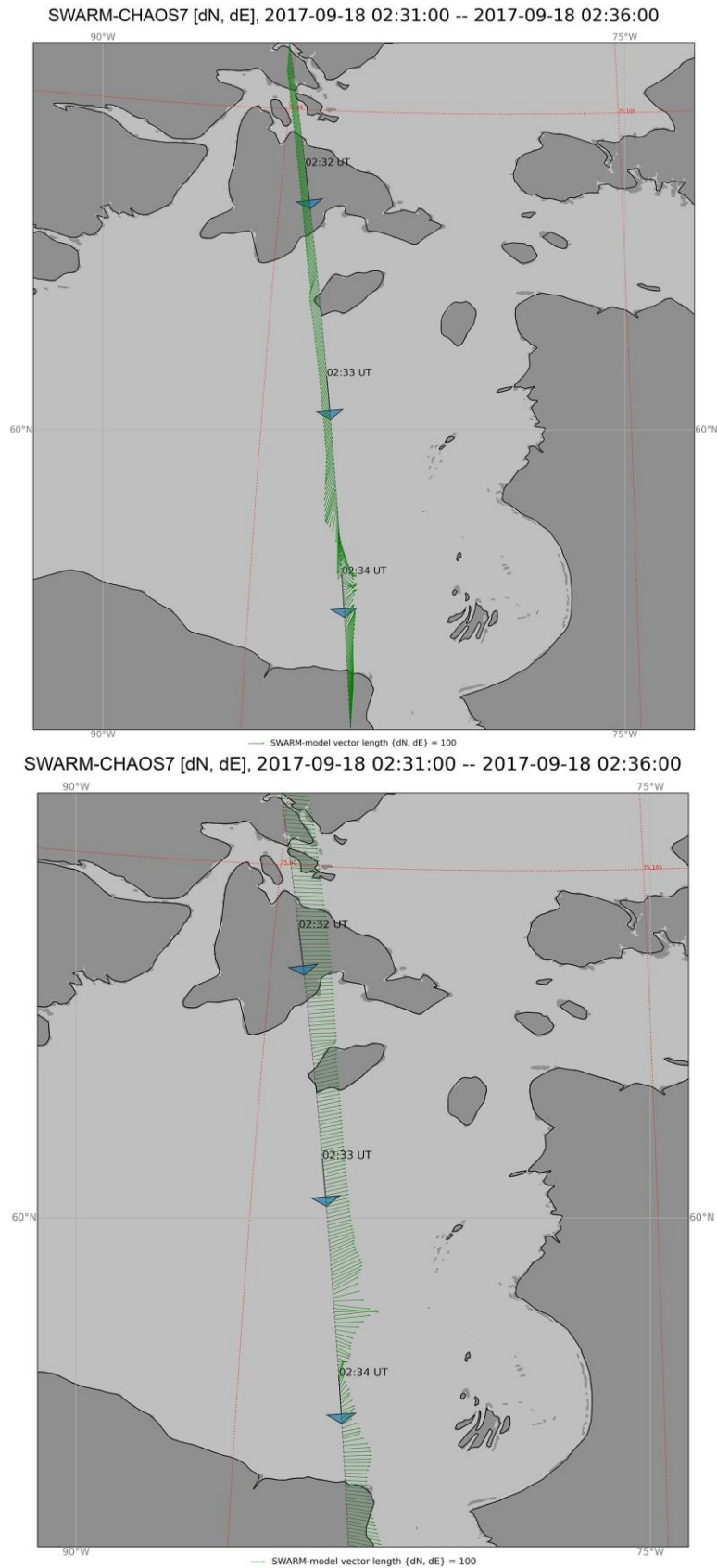


Figure 7. Perturbed vector field component $\Delta\mathbf{B}=\{\Delta N, \Delta E\}$ (green arrows) in the horizontal projection on September 18, 2017 at 02:31–02:36 UT in the user-selected region in the Miller projection (top); perturbed vector field component $\Delta\mathbf{B}=\{\Delta N, \Delta E\}$ (green arrows) in the projection of the field-line intersection point along the SWARM-A flight path (dashed line) on September 18, 2017 at 02:31–02:36 UT in the user-selected region in the Miller projection (bottom). The scale to the vector field is shown at the bottom; red dotted lines represent a grid of geomagnetic dipole coordinates

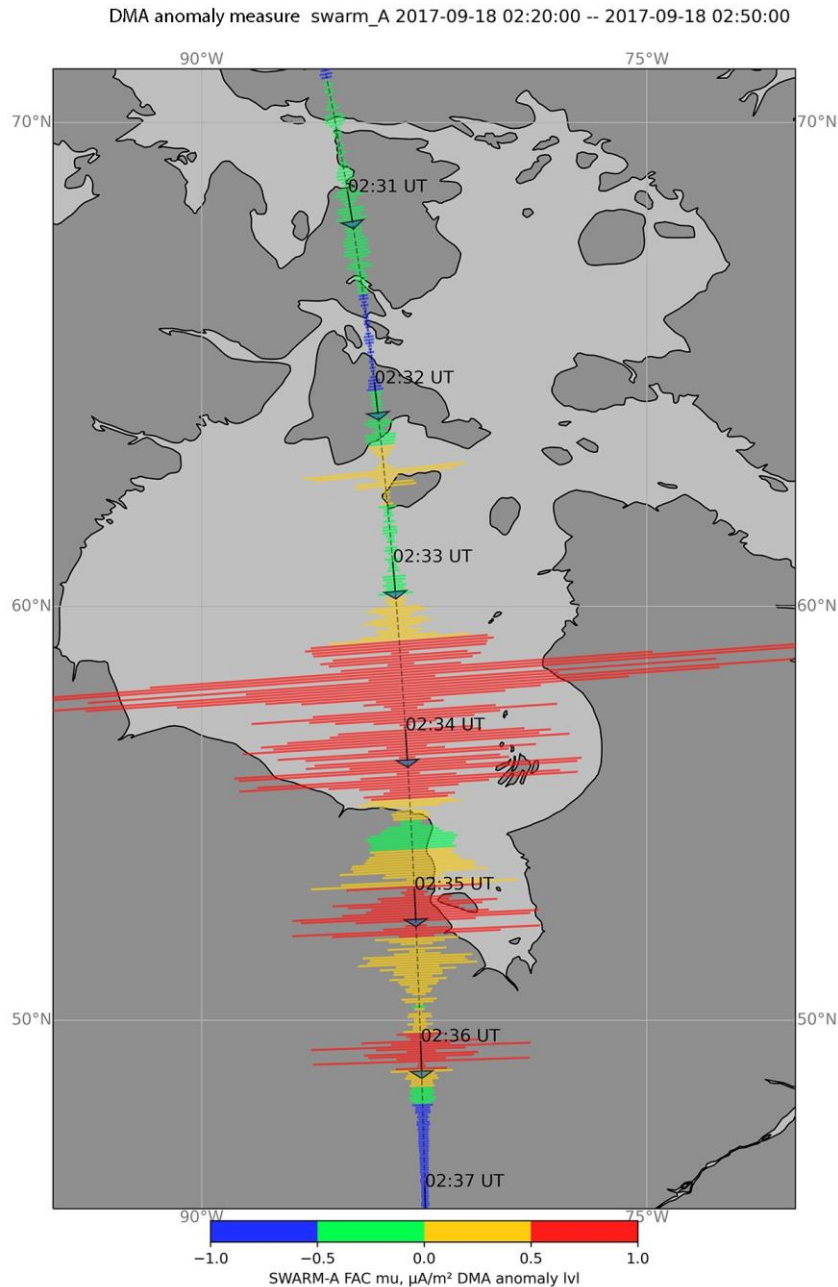


Figure 8. Classification of the FAC density in accordance with the DMA anomaly measure along the Swarm-A orbit (dashed line) on September 18, 2017 at 02:30–02:37 UT in the user-selected section of the Miller projection: the length of the transverse lines corresponds to the FAC density amplitude; the color indicates the anomaly measure $[-1, 1]$

analysis (DMA) — a series of algorithms aimed at tackling the main tasks related to data analysis: clustering and tracing in multidimensional arrays, morphological analysis of reliefs, search for anomalies and trends in records, etc. The algorithm used in this web system involves searching for anomalies in one-dimensional time series [Agayan et al., 2016]. Each value of the initial series is assigned a value from the interval $[-1, 1]$: the smaller the perturbed value from the time series analyzed, the closer it to -1 ; and the more anomalous the value, the closer it to 1 . Thus, the algorithm yields a new time series with a range of values $[-1, 1]$ and with the same domain of definition as in the original series. The algorithm relative to FAC density data is illustrated in Figure 8.

COMPARISON WITH THE VirES APPLICATION

A popular web service for visual analysis of Swarm satellite data is VirES (the Swarm Data Visualization Tool, [https://vires.services/]) of the European Space Agency and its web interface VRE (the Swarm Virtual Research Environment) [https://vre.vires.services/]. VirES is a highly interactive web interface for processing and searching for data from the archive of Swarm products and other auxiliary repositories. It includes multidimensional geographical visualization, interactive plotting, and processing tools for studying geomagnetic models and their temporal variations for comparison with direct satellite measurements in the

global context of space weather. Swarm data subsets, selected using universal filtering methods, can be loaded in various coding formats. The uploaded data can be combined according to different use cases. The system is convenient, first of all, due to the possibility of interactive analysis of satellite data on a three-dimensional globe directly in a web browser. In addition, VirES allows us to display the following satellite data:

- measurements of the total electron content (TEC) of the ionosphere with a 6 Hz frequency;
- plasma measurements (2 Hz) with a Langmuir probe, including electron temperature and plasma density;
- measurements of the equatorial electrojet on the day side.

VirES API also provides access to the following magnetic field measurements:

- hourly, minute, and second data from the INTERMAGNET ground-based observatories and the corresponding archive of the World Data Center for Geomagnetism of the British Geological Survey, as well as geomagnetic and solar activity indices (Dst , K_p , $F10.7$);
- data from virtual observatories for 1 and 4 months under the project of Geomagnetic Virtual Observatories (GVO);
- vector measurements of the magnetic field obtained from the CryoSat-2, GRACE, and GRACE-FO missions.

It is possible to combine additional geophysical layers on the map based on the following data:

- the model of the main geomagnetic field IGRF;
- the magnetic field model CHAOS-7 describing the contribution of the main, lithospheric, and magnetospheric fields;
- component-by-component difference between the satellite-measured geomagnetic field and the model field.

To access satellite data, it is possible to use the Heliophysics Application Programmer's Interface [<https://github.com/hapi-server>].

Thus, the TeslaSwarm system also has the basic functional for the VirES and HAPI applications. As mentioned above, effective FAC analysis requires transformation of the local coordinate system in which the magnetic field vector is measured. These applications, in contrast to the TeslaSwarm system, do not have the corresponding functional. Another advantage of the presented system is the ability to isolate Swarm passages within a given radius from the selected SuperMag network stations in order to compare ground and satellite observations of the magnetic field.

CONCLUSION

The online system largely saves the user from the most time-consuming work of choosing the moments of the satellite passage through a given region, calculating the satellite's ground path along Earth's surface, and converting data into a coordinate system oriented along the magnetic field. The system offers a more general insight into the geophysical conditions for the event

under study — position of the satellite relative to the auroral oval, background variations in the magnetic field, and ionospheric plasma density. The system is under development, and we will be grateful for any suggestions for its improvement.

The results reported in this paper have been obtained using data from geomagnetic observatories. We thank the team of the INTERMAGNET network for promoting high standards of functioning of geomagnetic observatories [<http://www.intermagnet.org>] and the team of the Interregional Geomagnetic Data Center [<http://geomag.gcras.ru>] for the free distribution of data online. The Swarm data is provided by the European Space Agency and is available at [<ftp://swarm-diss.esa.int>]. The SuperMag network data is available at [<https://supermag.jhuapl.edu/>]. The software implementation of the OP model is freely available at [<https://github.com/lkilcommons/OvationPyne>]. The NumPy and Pandas libraries are used for processing spatial data; and the Matplotlib-3.0 and Cartopy libraries, for rendering the visual part. The work employed data and services provided by the Shared Research Facility “Analytical Geomagnetic Data Center” of the Geophysical Center of the Russian Academy of Sciences. The work was financially supported by RSF (Grant No. 21-77-30010).

REFERENCES

- Agayan S., Bogoutdinov S., Soloviev A., Sidorov R. The study of time series using the DMA methods and geophysical applications. *Data Sci. J.* 2016, vol. 16, pp. 1–21. DOI: [10.5334/dsj-2016-016](https://doi.org/10.5334/dsj-2016-016).
- Alken P., Thébault E., Beggan C. D., Amit H., Aubert J., Baerenzung J., et al. International Geomagnetic Reference Field: the thirteenth generation. *Earth, Planets and Space.* 2021, vol. 73 (1), no 49. DOI: [10.1186/s40623-020-01288-x](https://doi.org/10.1186/s40623-020-01288-x).
- Dunlop M.W., Yang Y.Y., Yang J. Y., Lühr H., Shen C., Olsen N., et al. Multi-spacecraft current estimates at Swarm. *J. Geophys. Res.* 2015, vol. 120, iss.10, pp. 8307–8316.
- Finlay C.C., Kloss C., Olsen N., Hammer M. Toffner-Clausen L., Grayver A., et al. The CHAOS-7 geomagnetic field model and observed changes in the South Atlantic Anomaly. *Earth Planets and Space.* 2020, vol. 72. DOI: [10.1186/s40623-020-01252-9](https://doi.org/10.1186/s40623-020-01252-9).
- Forsyth C., Rae I.J., Mann I.R., Pakhotin I.P. Identifying intervals of temporally invariant field-aligned currents from Swarm: Assessing the validity of single-spacecraft methods. *J. Geophys. Res.: Space Phys.* 2017, vol. 122. DOI: [10.1002/2016JA023708](https://doi.org/10.1002/2016JA023708).
- Friis-Christensen E., Lühr H., Hulot G. Swarm: A constellation to study the Earth's magnetic field. *Earth, Planets and Space.* 2006, vol. 58, pp. 351–358.
- Gjerloev J. The SuperMAG data processing technique. *J. Geophys. Res.* 2012, no. 117, pp. A09213.
- Gvishiani A., Soloviev A., Krasnoperov R., Lukianova R. Automated hardware and software system for monitoring the Earth's magnetic environment. *Data Sci. J.* 2016, vol. 15, p.18. DOI: [10.5334/dsj-2016-018](https://doi.org/10.5334/dsj-2016-018).
- Kervalishvili G., Park J. Swarm L2 FAC-single product description. Swarm Expert Support Laboratories (5). 2017. https://cloud.gcras.ru/d/s/vsgRgEVWNkjjvy7GDefXCxVkrT2Byy1EW/8FO5KX4RT-szECaxtrtGLod5pXAvJzZt-_rvgPhG-3wo.

Lühr H., Park J., Gjerloev J.W., Rauberg J., Michaelis I., Merayo M.G., Brauer P. Field-aligned currents' scale analysis performed with the Swarm constellation. *Geophys. Res. Lett.* 2015, vol. 42, pp. 1–8. DOI: [10.1002/2014GL062453](https://doi.org/10.1002/2014GL062453).

Lühr H., Ritter P., Kervalishvili G., Rauberg J. Applying the dual-spacecraft approach to the Swarm constellation for deriving radial current density. *Ionospheric Multi-Spacecraft Analysis Tools. ISSI Scientific Report Series*, Springer, Cham. 2020, Vol. 17. DOI: [10.1007/978-3-030-26732-2_6](https://doi.org/10.1007/978-3-030-26732-2_6).

Machol J.L., Green J.C., Redmon R.J., Viereck R.A., Newell R.T. Evaluation of OVATION Prime as a forecast model for visible aurora. *Space Weather*. 2012, no. 10, S03005. DOI: [10.1029/2011SW000746](https://doi.org/10.1029/2011SW000746).

Neubert T., Christiansen F. Small-scale, field-aligned currents at the top-side ionosphere. *Geophys. Res. Lett.* 2003, vol. 30, p. 2010. DOI: [10.1029/2003GL017808](https://doi.org/10.1029/2003GL017808).

Newell P.T., Liou K., Zhang Y., Sotirelis T., Paxton L.J., Mitchell E.J. OVATION Prime-2013: Extension of auroral precipitation model to higher disturbance levels. *Space Weather*. 2014, vol. 12, pp. 368–379. DOI: [10.1002/2014SW001056](https://doi.org/10.1002/2014SW001056).

Papitashvili V. O., Christiansen F., Neubert T. A new model of field-aligned currents derived from high-precision satellite magnetic field data. *Geophys. Res. Lett.* 2002, vol. 29, p. 1683.

Park J., Lühr H., Knudsen D.J., Burchill J.K., Kwak, Y.-S. Alfvén waves in the auroral region, their Poynting flux, and reflection coefficient as estimated from Swarm observations. *J. Geophys. Res.* 2017, vol. 122, pp. 2345–2360. DOI: [10.1002/2016JA023527](https://doi.org/10.1002/2016JA023527).

Pilipenko V.A. Space weather impact on ground-based technological systems. *Solnechno-zemnaya fizika* [Solar-terrestrial physics], 2021, vol. 7, no. 3, pp. 73–110. (In Russian). DOI: [10.12737/szf-73202106](https://doi.org/10.12737/szf-73202106).

Pilipenko V., Heilig B. ULF waves and transients in the topside ionosphere, in: “Low-frequency Waves in Space Plasmas”. *Geophysical Monograph. Ser.* 2016. vol. 216, pp. 15–29. Wiley/AGU DOI: [10.1002/9781119055006](https://doi.org/10.1002/9781119055006).

Ritter P., Lühr H., Rauberg J. Determining field-aligned currents with the Swarm constellation mission. *Earth Planets and Space*. 2013, vol. 65, iss. 11, pp. 1285–1294.

Russell C.T., Snare R.C., Means J.D., Pierce D., Dearborn D., Larson M., et al. The GGS/POLAR magnetic fields investigation. *Space Sci*, 1995, vol. 71, pp. 563–582.

Swarm Level 2 Processing System Consortium, Product specification for L2 Products and Auxiliary Products, Doc.no: SW-DS-DTU-GS-0001. 2019, p. 100.

Tsyganenko N.A. A magnetospheric magnetic field model with a warped tail current sheet. *Planet. Space Sci.* 1989, vol. 37, pp. 5–20. DOI: [10.1016/0032-0633\(89\)90066-4](https://doi.org/10.1016/0032-0633(89)90066-4).

Tøffner-Clausen L. Swarm level 1b product definition. SW-RS-DSC-SY-0007. 2021, iss. 5.26. [Available at https://cloud.gcras.ru/d/s/vsgRgEVWNkjvy7GDefXCxVkrT2Byy1EW/8FO5KX4RT-szECaxtrtgLOd5pXAvJzZt-_rvgPhG-3wo..]

Vobobev A.V., Soloviev A.A., Pilipenko V.A., Vorobeva G.R. Interactive computer model for aurora forecast and analysis. *Solar-Terr. Phys.* 2022, vol. 8, no. 2, pp. 84–90. DOI: [10.12737/stp-82202213](https://doi.org/10.12737/stp-82202213).

Wu J., Knudsen D.J., Gillies D.M., Donovan E.F., Burchill J.K. Swarm observation of field-aligned currents associated with multiple auroral arc systems. *J. Geophys. Res.* 2017, vol. 122. DOI: [10.1002/2017JA024439](https://doi.org/10.1002/2017JA024439).

Zanetti L.J., Anderson B.J., Potemra T.A., Clemmon J. H., Wilmingham J.D., Sharbe J.R. Identification of auroral oval boundaries from in situ magnetic field measurements. *J. Geophys. Res.* 1998, vol. 103, p. 4187.

URL: <http://aleph.gcras.ru/teslaswarm> (accessed November 3, 2023).

URL: <http://ckp.gcras.ru> (accessed November 3, 2023).

URL: <https://pypi.org/project/PyMySQL/> (accessed November 3, 2023)

URL: <ftp://swarm-diss.eo.esa.int> (accessed November 3, 2023).

URL: <https://ccmc.gsfc.nasa.gov/models/Ovation-Prime~2.3> (accessed November 3, 2023).

URL: <https://supermag.jhuapl.edu> (accessed November 3, 2023).

URL: <https://pypi.org/project/igrfu> (accessed November 3, 2023).

URL: <https://pypi.org/project/chaosmagpy> (accessed November 3, 2023).

URL: <https://omniweb.gsfc.nasa.gov/> (accessed November 3, 2023).

URL: <https://vires.services/> (accessed November 3, 2023).

URL: <https://vre.vires.services> (accessed November 3, 2023).

URL: <https://github.com/hapi-server> (accessed November 3, 2023).

URL: <http://www.intermagnet.org> (accessed November 3, 2023).

URL: <http://geomag.gcras.ru> (accessed November 3, 2023).

URL: <https://github.com/lkilcommons/OvationPyme> (accessed November 3, 2023).

Original Russian version: Belov I.O., Soloviev A.A., Pilipenko V.A., Dobrovolsky M.N., Bogoutdinov SH.R., Kalinkin K.D., published in *Solnechno-zemnaya fizika*. 2023. Vol. 9. Iss. 4. P. 121–133. DOI: [10.12737/szf-94202314](https://doi.org/10.12737/szf-94202314) © 2023 INFRA-M Academic Publishing House (Nauchno-Izdatelskii Tsentr INFRA-M)

How to cite this article

Belov I.O., Soloviev A.A., Pilipenko V.A., Dobrovolsky M.N., Bogoutdinov SH.R., Kalinkin K.D. Online system for analyzing currents in the upper ionosphere according to Swarm satellite data. *Solar-Terrestrial Physics*. 2023. Vol. 9. Iss. 4. P. 111–122. DOI: [10.12737/stp-94202314](https://doi.org/10.12737/stp-94202314).